



# Control strategy for a hydrogen combustion engine with lean and stoichiometric combustion system

Katrin Himmelseher<sup>1</sup> · Alexander Lampkowski<sup>1</sup> · Stefan Sterlepper<sup>1</sup> · Volker Müller<sup>2</sup> · Carole Querel<sup>3</sup> · Joschka Schaub<sup>2</sup> · Dennis Lorei<sup>2</sup> · Olaf Brüning<sup>2</sup> · Claudia Conée<sup>4</sup> · Helmut Ruhland<sup>4</sup> · Marco Günther<sup>1</sup> · Stefan Pischinger<sup>1</sup>

Received: 28 October 2025 / Accepted: 3 November 2025 / Published online: 2 December 2025  
© The Author(s) 2025

## Abstract

Hydrogen presents a promising opportunity for the reduction of CO<sub>2</sub> emissions in combustion processes. Due to its wide ignition limits, operation in lean mode is possible, which significantly reduces NO<sub>x</sub> emissions. However, this lean operation also leads to a reduction in the resulting torque. In contrast, stoichiometric operation increases maximum power output but leads to increased NO<sub>x</sub> emissions. In particular, a cost-effective three-way catalyst can be used in stoichiometric operation, enabling effective emission control. This investigation proposes an innovative approach that involves lean-burn operation at part load conditions and switching to stoichiometric operation at full load. The transition between these two modes has a considerable impact on overall NO<sub>x</sub> emissions. To optimize this process, new functions were developed that implement countermeasures such as lambda control, ignition timing adjustment, catalyst purging, and shortening the switching range through the use of variable valve timing and variable turbine geometry. The results show that nitrogen oxide (NO<sub>x</sub>) emissions downstream of the three-way catalyst are kept below  $c_{\text{NO}_x} = 100$  ppm in the lean operating range and below  $c_{\text{NO}_x} = 30$  ppm in the stoichiometric operating range. By optimizing the transition between the two operating modes and using advanced emission control technologies, it is possible to reduce NO<sub>x</sub> emissions by 84% while maintaining power efficiency under different load conditions. In addition, the almost torque-neutral switching between the two operational modes ensures that the vehicle's drivability is not impaired. By incorporating additional dosing of a urea-water solution in an active SCR system, a significant improvement in NO<sub>x</sub> reduction is attained, achieving levels comparable to those of diesel internal combustion engines. This dual-mode operation strategy improves the feasibility of hydrogen as a viable fuel alternative in future energy systems.

**Keywords** Hydrogen combustion engine · Lean operation · Stoichiometric operation · Control functions · NO<sub>x</sub> emissions · Exhaust aftertreatment

## Abbreviations

$c_{\text{NO}_x}$  NO<sub>x</sub> concentration  
 $\Delta_{\text{NO}_x}$  NO<sub>x</sub> difference over WLTC tests  
 $\text{EF}_{\text{NO}_x}$  NO<sub>x</sub> EF, related to driving cycle

$\eta_{\text{NO}_x}$	NO <sub>x</sub> conver
FTIR	Fourier-transform-infrared-spektroskopie
FID	Flame ionization detector
GHSV	Gas hourly space velocities
H <sub>2</sub>	Hydrogen
H <sub>2</sub> O	Water
$\lambda$	Air–fuel ratio
$\lambda_{\text{Des, Stationary}}$	Stationary desired air–fuel ratio
NDIR	Nondispersive infrared sensor
NH <sub>3</sub>	Ammonia
NO	Nitric oxide
NO <sub>2</sub>	Nitrogen dioxide
NO <sub>x</sub>	Nitrogen oxides (NO and NO <sub>2</sub> )
O <sub>2</sub>	Oxygen

✉ Katrin Himmelseher  
himmelseher@tme.rwth-aachen.de

<sup>1</sup> Thermodynamics of Mobile Energy Conversion Systems, RWTH Aachen University, Aachen, Germany

<sup>2</sup> FEV Europe GmbH, Aachen, Germany

<sup>3</sup> FEV France, Trappes, France

<sup>4</sup> Ford-Werke GmbH, Cologne, Germany

PMD	Polarization mode dispersion
SCR	Selective catalytic reduction
SGB	Synthetic gas test bench
$T_{\text{Inlet}}$	Inlet catalyst temperature
TWC	Three-way catalyst
VTG	Variable turbine geometry
VVT	Variable valve time
WLTC	Worldwide harmonized light vehicles test cycle
$\psi_{\text{H}_2\text{O}}$	$\text{H}_2\text{O}$ emissions
$\psi_{\text{NO}_x}$	$\text{NO}_x$ emissions
$x_{\text{NO}_2/\text{NO}_x}$	$\text{NO}_2/\text{NO}_x$ ratio

## 1 Introduction

Hydrogen combustion engines represent an innovative technology that enables the use of existing infrastructures and technologies of conventional internal combustion engines while leveraging the benefits of hydrogen as a clean fuel [14, 33]. These engines could not only contribute to greenhouse gas emission reductions but also meet the growing demand for flexible and efficient propulsion systems in an evolving mobility landscape. Especially for applications that are difficult to electrify, such as commercial vehicles, agricultural machinery and existing fleets, the hydrogen combustion engine represents a promising technology.

Hydrogen as a fuel is characterized by a high flame speed and rapid heat diffusion, which leads to very fast combustion [34]. Recent advances in hydrogen combustion engine technology focus on improving efficiency [16, 22, 37], performance [20], and emissions control [24, 36, 37]. Researchers and manufacturers are exploring innovative designs to improve the combustion process, for example, by optimizing fuel injection systems [9, 13] and using advanced ignition techniques [26, 40]. Several automotive manufacturers and suppliers are currently testing prototype vehicles and machines powered by hydrogen combustion engines, showing promising results in terms of power output and drivability [17, 28]. Furthermore, industry, stakeholders and research institutions aim to address the infrastructural challenges associated with hydrogen refueling stations, facilitating the broader adoption of this technology [7, 8, 10]. As these developments progress, hydrogen combustion engines will play a critical role in realizing sustainable transportation solutions.

Most hydrogen combustion engine designs exploit the favourable flammability limits of hydrogen to operate the engine in lean-burn mode. The lean-burn operation strategy offers several advantages that affect both engine efficiency and emissions [3, 22, 25, 29, 32, 37]. One of the main benefits of lean-burn operating is the reduction of

combustion temperatures, as the excess air cools the combustion temperature and inhibits  $\text{NO}_x$  formation [1, 34]. The reduced combustion temperatures also help minimize the risk of knocking and pre-ignition, which can occur at higher temperatures ( $\lambda < 2$ ) [18, 22]. Another advantage is improved energy efficiency [32]. Operating with a lean mixture enables lower engine fuel consumption because more energy can be extracted from the available hydrogen [6, 41]. However, implementing a lean-burn operation strategy presents challenges. Although the rapid release of combustion energy and rapid combustion leads to the high efficiency mentioned above, the lean-burn concept also leads to reduced power output, as Karim [15] shows.

Stoichiometric operation of hydrogen combustion engines enables maximum power output because more fuel can be burned per cycle compared to lean combustion. Misul et al. [20] show higher BMEP during stoichiometric operation compared to a lean-burn ( $\lambda = 2$ ) operation. Operating the engine in stoichiometric mode results in high pressure and temperature gradients, which can increase the likelihood of pre-ignition and knocking. This is influenced by the combustion speed, which significantly affects the performance of a hydrogen engine [18]. The very high flame speed causes rapid combustion, resulting in high flame temperature and short quenching distance [3]. Consequently, this raises the tendency for knocking, as well as material stress and noise emissions. Maintaining a stoichiometric operation also improves the performance of conventional exhaust after-treatment systems for emission reduction, such as three-way catalysts. This improves overall emission control by ensuring that any remaining pollutants are effectively converted into less harmful compounds before being released into the atmosphere [39]. However, achieving and maintaining a stoichiometric mixture in hydrogen combustion engines requires precise control of the fuel injection and air intake systems.

Another option is dual-mode operation, which achieves the benefits of lean operation at low- and part-load, while using a stoichiometric air–fuel-ratio at high-load to combine all positive effects. Dual-mode strategies have been investigated by BMW and Ferrari, again with a focus on high performance and low emissions [5, 19, 27, 35]. Rottengruber et al. investigated a three-zone concept with lean operation at low load, in which the air/hydrogen mixture is generated by external mixture formation. At part load, the engine switches to external mixture formation with a stoichiometric air–fuel-ratio, and at high load, it switches to internal mixture formation, also with stoichiometric air–fuel ratio. The strategy was tested on a single-cylinder research engine and showed that an even higher IMEP can be achieved than for comparable gasoline engines. The limit for  $\text{NO}_x$  emissions was set at 2.2 vol% [27]. Wallner et al. [35] also investigated a switching

strategy in a BMW Hydrogen 7 vehicle with lean operation at low load and stoichiometric operation at high load. For stoichiometric operation, they used a combination of a three-way catalyst and a  $\text{NO}_x$  storage catalyst and achieved very low  $\text{NO}_x$  emissions. Also Medda et al. [19] also report lean and stoichiometric operation to combine the advantages of both strategies. In particular, the challenge of switching between the two operating modes is addressed in the presented project.

## 2 Leveraging engine hardware to enable advanced operating strategies

The engine described in this paper is a three-cylinder gasoline direct injection engine that has been modified for use with hydrogen, but not fully optimized. The engine features variable valve timing (VVT), variable turbine geometry (VTG), a three-way catalyst, and high-pressure exhaust gas recirculation (EGR) to adapt the operation strategy. The complete setup is described by Terhorst-Kluge et al. [31].

The synthetic gas test bench (SGB) enables the precise dosing of a wide range of gases to characterize catalyst samples under conditions that offer significantly higher reproducibility compared to engine test benches. Catalyst samples are drilled from the monolith and mounted in the test bench. By adjusting the volumetric flow rate and sample length, a wide range allows for the investigation of a broad range of gas hourly space velocities (GHSV) can be investigated. Gas dosing is controlled via mass flow controllers and solenoid valves. Heaters ensure temperature control according to predefined ramps. In addition, emission analysis is a central aspect of the test bench. Emissions are quantified both upstream and downstream of the catalyst sample using various techniques, including FTIR, FID, NDIR, PMD, and a hydrogen mass spectrometer (HSense). A detailed overview and description of the SGB setup can be found in previously published papers [23, 38].

The goal of the project is to achieve high-power output while simultaneously keeping the  $\text{NO}_x$  emissions at a very low level. The projected engine map is therefore divided into three zones: A quality control zone for fuel-guided lean-burn operation at low and part load, a quantity control zone for air-guided stoichiometric operation at high-load, and a transition zone for switching between lean and stoichiometric operation (Fig. 1).

Due to the lower temperatures during lean operation, the  $\text{NO}_x$  emissions are very low [27]. However, closer to the stoichiometric area, the emissions rise significantly (Fig. 1). To take advantage of the beneficial power yield of stoichiometric operation at full load, countermeasures to reduce  $\text{NO}_x$  emissions must be considered. Here, the three-way

catalyst mentioned above shows effective  $\text{NO}_x$  conversion down to single-digit ppm values.

Between the two low  $\text{NO}_x$  emission ranges, there is a range ( $\lambda > 1$  &  $\lambda < 2.4$ ) where high emissions occur. To avoid  $\text{NO}_x$  emission peaks during the transition, it is very important to cross this area very fast. At the same time, the transition between the modes must be torque-neutral to avoid any impact on the drivability. To achieve this, the installed hardware can be used. The VTG systems adjust the geometry of the turbocharger turbine blades to optimize airflow. VVT allows a faster actuation of the air path than the throttle flap. The technology enables the optimization of the timing of intake valve opening and closing to improve engine performance. By simultaneously adjusting timing and valve lift, VVT helps adjust the air mass flowing into the cylinder. The desired opening and closing angle of intake valves is stored based on maps derived from measurements conducted on the test bench, thus enabling precise adjustments to different engine conditions.

The specific valve lift is directly derived from these timings and the engine speed (Fig. 2). The valve timing significantly influences the filling process, as it affects calculations for residual gas and valve overlap. A different configuration can lead to distinct interactions between the intake and exhaust phases and influence the overall engine behavior. Therefore, incorporating these variations into the filling model was crucial for achieving precise control. Another critical aspect that needed attention was the choke effect. This phenomenon must be considered because it depends on several variables, including valve timing, valve lift and the operation mode of the engine. To estimate the air charge, the actual valve timing is used as feedback from the VVT system in a physical air charge model to ensure accurate modelling of the intake flow. At the same time, target valve timing from test bench measurements is used to determine the intake pressure using an inverted model of the air charge estimation. The resulting intake manifold pressure is controlled by adjusting the intake throttle position using model-based pre-control and a PI governor. The boost pressure is controlled by adjusting the VTG position using a real-time capable turbocharger model. As a result of these considerations, we successfully integrated a map-based pre-control for the valve timing system, tailored to both operating modes. This approach enables enhanced adaptability leading to improved performance and reduced emissions.

Full valve lift is used primarily at maximum engine power to ensure full performance when needed. In the part load range, however, early closing of the intake valve is used. This adjusts the amount of air supplied to the cylinder according to the torque curve [11].

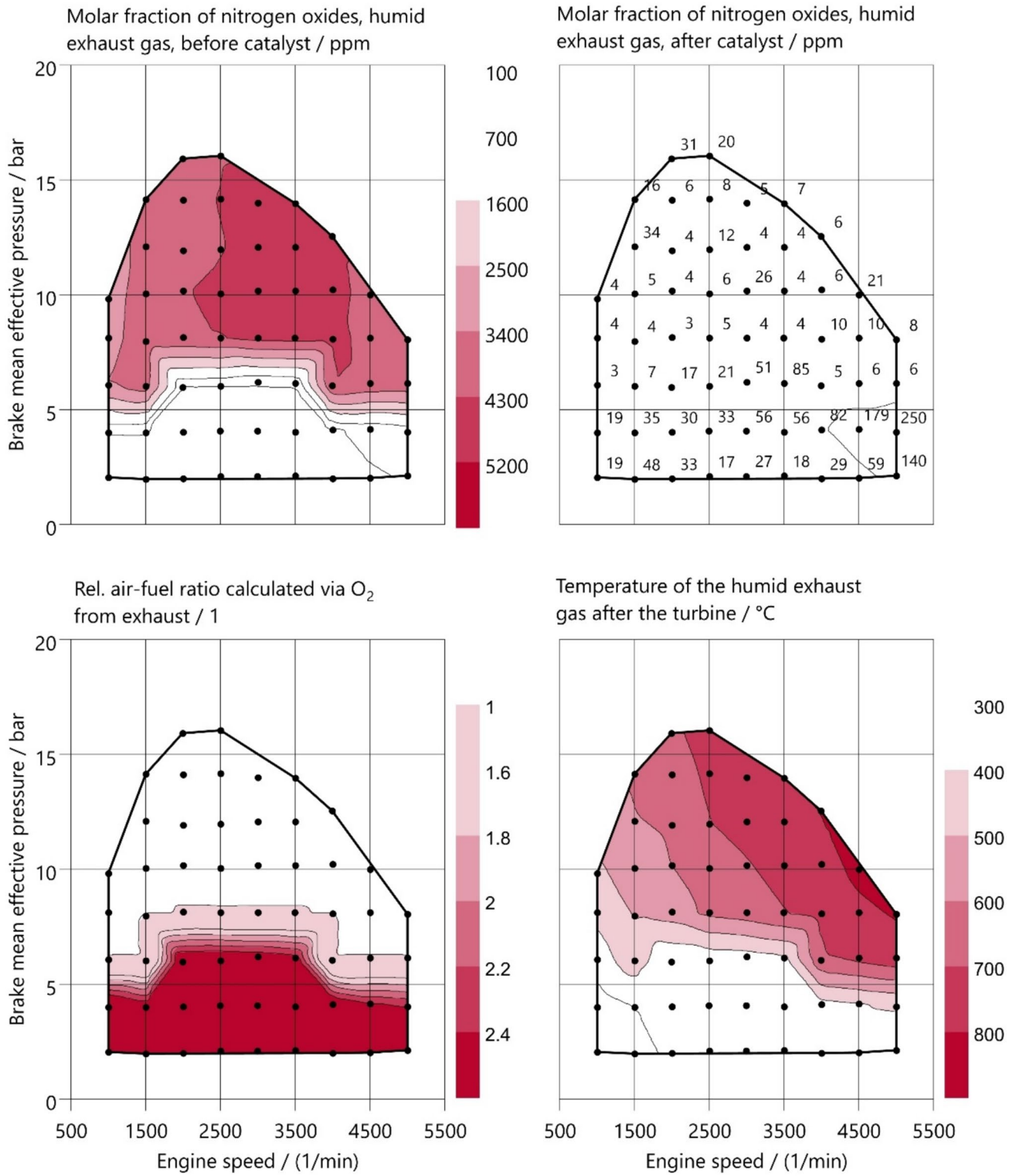


Fig. 1 Engine maps for NO<sub>x</sub> emissions before and after catalyst, air–fuel ratio and exhaust temperature

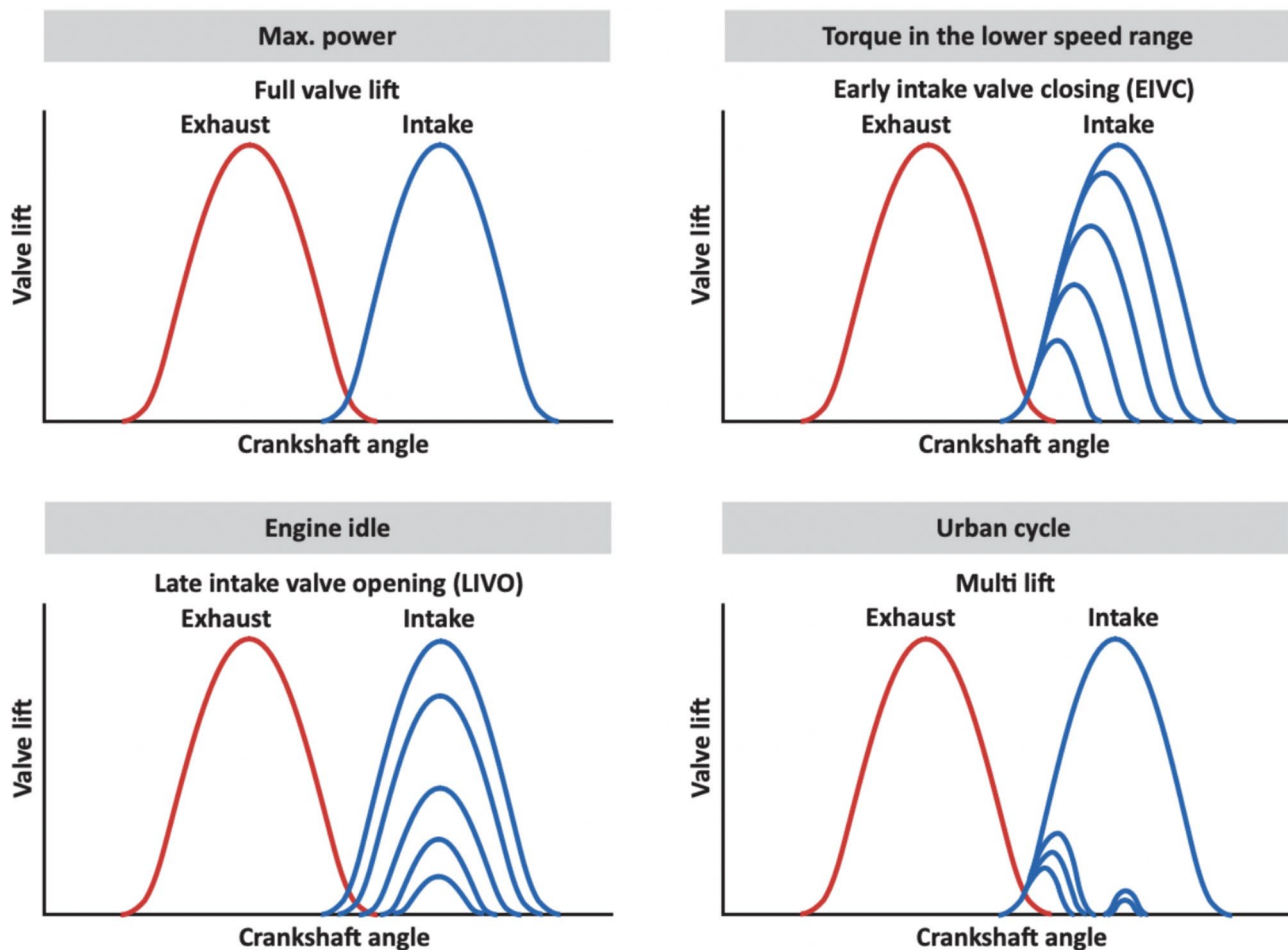


Fig. 2 Working principle of the UniAir-System [11]

### 3 Testing and validation of the dual-mode operation with switching between lean and stoichiometric operation

Figure 3 shows a schematic of the operating mode change. Starting from lean-burn operation, an open loop lambda control is used because the lambda sensor is highly cross-sensitive to residual hydrogen in the exhaust gas [30]. In stoichiometric operation, a closed-loop lambda control is also possible. In the case of a negative load ramp, the change between operating modes can be achieved directly by adjusting the fuel mass. With a positive load ramp, however, both the intake pressure and the air mass must be reduced. The target full mass is calculated in both operating modes. In stoichiometric operation, the target air–fuel-ratio is set to one, so the target air mass can be calculated directly from desired air–fuel-ratio and the desired fuel mass. Once the stationary air–fuel-ratio has been reached, the closed-loop controller can be activated. The air–fuel-ratio is adjusted using a correction factor of the fuel mass. The desired air–fuel-ratio

is limited to a minimum to prevent  $\text{NO}_x$  emissions during stationary operation and to a maximum to prevent misfires. In lean operation, however, the desired lambda value is calculated from a limited desired fuel mass. The boundary conditions are a maximum air–fuel-ratio to avoid misfires and a minimum air–fuel-ratio to avoid high  $\text{NO}_x$  emissions during stationary operation. In the next step, the target air mass can be determined from the desired air–fuel-ratio. Implementation of the procedure under realistic operating conditions results in high  $\text{NO}_x$  emission peaks when switching from lean operation to stoichiometric. Although the duration of this peak is very short, the cumulative emissions in a WLTC cycle are very high with 15.34 g per cycle, corresponding to  $\text{EF}_{\text{NO}_x} = 660 \text{ mg/km}$  (Fig. 4). To reduce the peaks, optimizations of the switching strategy are integrated into the software. First, the parameters of the lambda controller were adjusted to achieve a faster response and avoid areas where the three-way catalyst is not working efficiently. Second, a wobble-function [2], familiar from modern gasoline engines, was integrated to improve catalyst efficiency in stoichiometric operation. Figure 5 shows a load step that

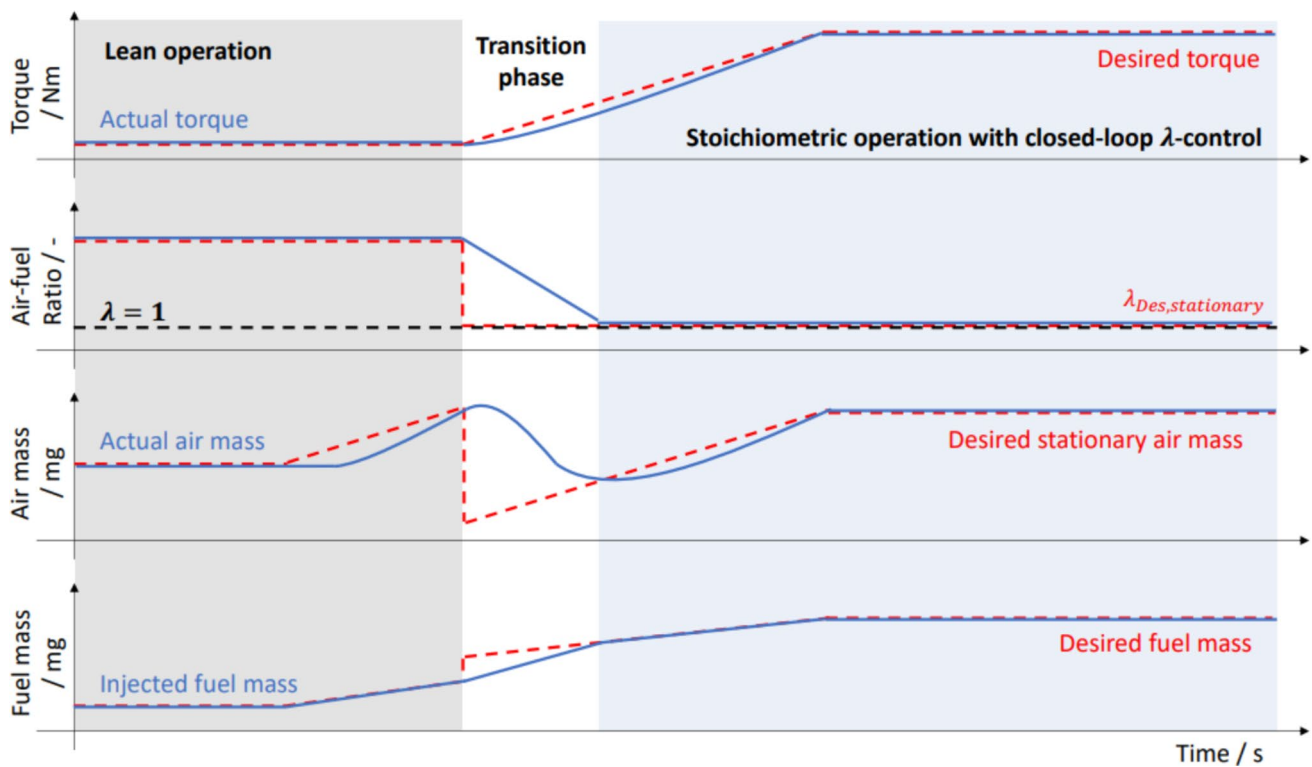


Fig. 3 The dual-mode strategy [12]

includes such a wobble-function with a mean air-fuel-ratio of  $\lambda = 0.97$ . Furthermore, enriching the air-fuel mixture generally reduces the  $\text{NO}_x$  emissions. The engine runs very stable and without knocking with a slightly rich mixture. However, this causes high ammonia emissions, which are caused by the three-way catalyst [4]. For this reason, the mean air-fuel-ratio of the wobble function has been raised to the usual value of  $\lambda = 1$ .

After switching from lean to rich, the oxygen storage capacity of the three-way catalyst is fully utilized, deactivating it for  $\text{NO}_x$  reduction. To optimize the efficiency of the catalyst under these dynamic conditions, a purge function is integrated. A brief enrichment of the mixture helps to remove oxygen from the catalyst, allowing for a faster, high-performance average oxygen storage loading and the desired catalyst efficiency.

As an additional measure, adjusting the ignition angle by lowering the temperature can contribute to reducing  $\text{NO}_x$  emission [21]. Figure 6 illustrates the transition between lean and stoichiometric combustion modes during a load ramp; an adjustment of the ignition timing can be observed. The diagram illustrates the impact on  $\text{NO}_x$  emissions. It also shows the low  $\text{NH}_3$  emissions achieved through optimized control of the air-fuel ratio.

The integration of all these developed functions into the software leads to a reduction of accumulated  $\text{NO}_x$  emissions of 2.38 g per cycle, corresponding to

$\text{EF}_{\text{NO}_x} = 102 \text{ mg/km}$  (Fig. 7). Despite the significant reduction in  $\text{NO}_x$  peaks during the transition from lean to stoichiometric operation, residual  $\text{NO}_x$  peaks continue to occur at these switchover points. To further reduce these emissions, ongoing optimization efforts are focused on accelerating the switchover transitions.

Overall, the WLTC cycle test in Fig. 8 shows a  $\text{NO}_x$  emission reduction of  $\Delta_{\text{NO}_x} = 84\%$  compared to the original WLTP emissions in Fig. 5. The individual contributions to this result are illustrated in Fig. 8. The resulting  $\text{NO}_x$  emissions of  $\text{EF}_{\text{NO}_x} = 102 \text{ mg/km}$  are still above the legal limit, so further optimization should follow. On the one hand, there is the possibility to control the VVT system to accelerate the transition process. On the other hand, the high-pressure EGR integrated into the hardware can be used to enlarge the lean operation area. When switching from a lower air-fuel ratio to the stoichiometric area, the transition area would be smaller, which also accelerates the transition and reduces the  $\text{NO}_x$  emissions. However, the combustion engine hardware has not been fully optimized for hydrogen. Modifications to the combustion chamber and thus to the mixture formation would lead to further homogenization in a series engine. This should reduce the raw emissions and, accordingly, the tailpipe emissions.

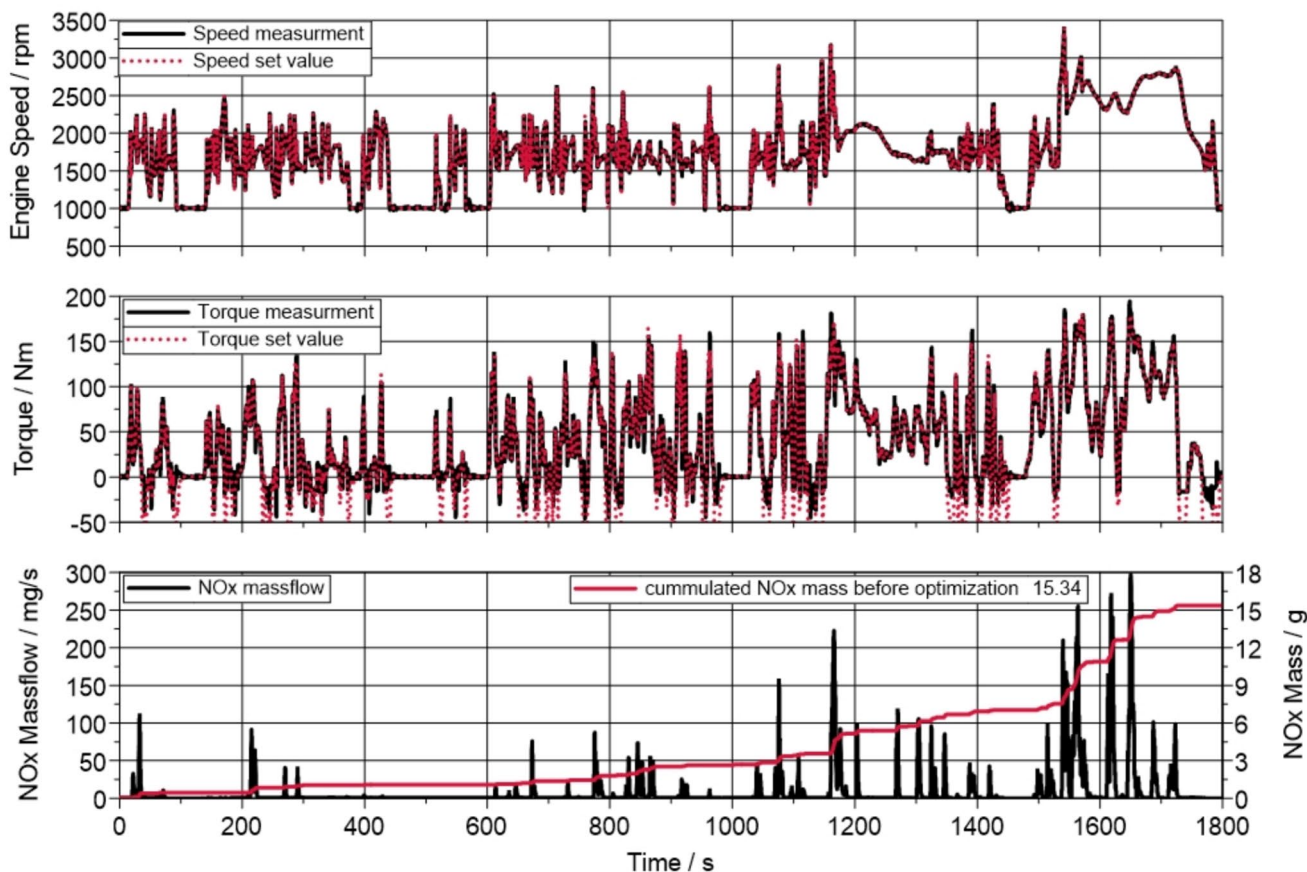


Fig. 4 WLTC without strategy optimization

#### 4 Aftertreatment

While the TWC enables high  $\text{NO}_x$  conversion efficiency  $\eta_{\text{NO}_x}$  under stoichiometric engine operation, and engine calibration strategies can further reduce  $\text{NO}_x$  raw emissions, there may be additional reduction potential during lean operation and the transition phases between stoichiometric and lean modes. This raises the question: Can an additional catalyst downstream of the TWC further reduce  $\text{NO}_x$  tailpipe emissions without significantly increasing system cost and complexity? A passive selective catalytic reduction (SCR) catalyst could offer such potential by utilizing secondary emissions such as  $\text{NH}_3$ , formed above the TWC. In this concept, the  $\text{NH}_3$  generated under rich conditions and during switchover phases can be stored on the SCR catalyst and subsequently used to reduce  $\text{NO}_x$  during lean operation. Figure 9 illustrates the  $\text{NO}_x$  conversion efficiency  $\eta_{\text{NO}_x}$  of a Cu-SSZ-13 catalyst as a function of catalyst inlet temperature  $T_{\text{Inlet}}$  at two  $\text{NO}_2/\text{NO}_x$  ratios of  $x_{\text{NO}_2/\text{NO}_x} = 0$  and 0.5. The lower efficiency  $\eta_{\text{NO}_x}$  observed at  $x_{\text{NO}_2/\text{NO}_x} = 0$  compared to  $x_{\text{NO}_2/\text{NO}_x} = 0.5$  underscores the strong temperature-dependent sensitivity to the  $\text{NO}_2/\text{NO}_x$  ratio. Nevertheless, at a temperature above  $T_{\text{Inlet}} > 230$  °C,  $\text{NO}_x$

conversion efficiencies above  $\eta_{\text{NO}_x} \geq 99\%$  are achieved in both cases.

The characterization of the SCR catalyst suggests significant potential for additional  $\text{NO}_x$  reduction when implemented downstream of the TWC. However, the extent of  $\text{NO}_x$  conversion is limited by the amount of  $\text{NH}_3$  produced by the TWC. The question remains: How much potential does a passive SCR really offer under the operating conditions investigated during the WLTC? Predictive simulations show that the potential for  $\text{NO}_x$  reduction with a downstream passive SCR with a volume of  $V_{\text{SCR}} = 1$  l operating under the shown strategy is less than 1% improvement over the cycle compared to TWC-only operation. This is due to the limited quantities of  $\text{NH}_3$  generated relative to the  $\text{NO}_x$  concentration. Likewise, a tested engine operating strategy with increased  $\text{NH}_3$  formation led to higher  $\text{NO}_x$  emissions, which results in only a minor overall improvement in  $\text{NO}_x$  reduction. Efficient  $\text{NO}_x$  reduction with a passive SCR system would require an operation strategy that is fully optimized to produce the right amount of  $\text{NH}_3$  emissions. In contrast, when considering an active  $\text{NH}_3$ -SCR system with demand-controlled dosing of urea-water solution, the measured tailpipe  $\text{NO}_x$  emissions in the WLTC can be

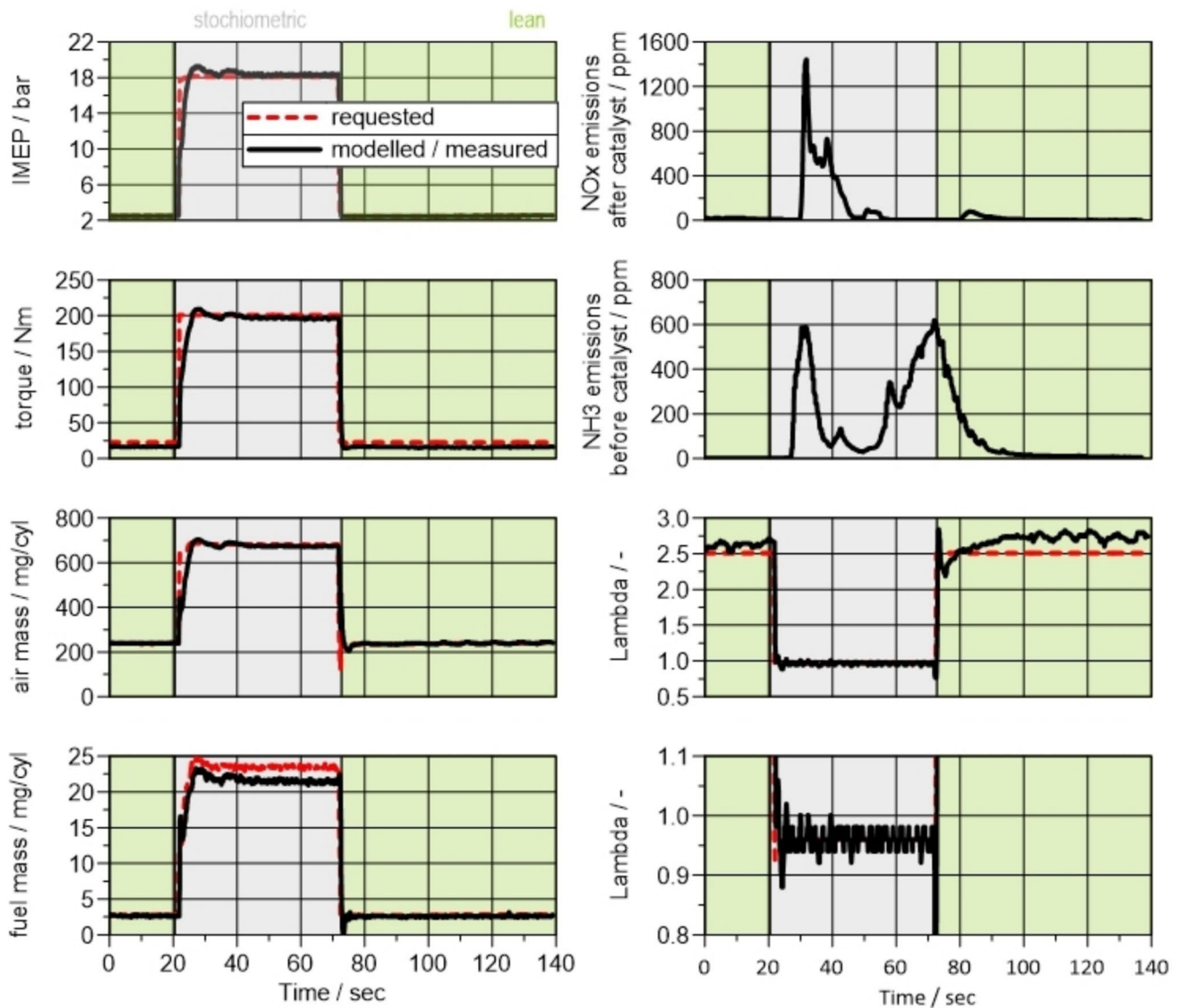


Fig. 5 Load step with wobble function

further reduced by up to 90% compared to the TWC-only configuration.

In conclusion, utilizing the  $\text{NH}_3$  formed in the TWC in a passive SCR contributes to the reduction of  $\text{NH}_3$  tailpipe emissions. However, under the engine operating conditions investigated, the application of a passive SCR in addition to the TWC does not lead to the desired improvement. In contrast, in combination with the additional dosing of a urea-water solution in an active  $\text{NH}_3$ -SCR system, a substantial enhancement in  $\text{NO}_x$  reduction is achieved, reaching values comparable to those of lean-burn  $\text{H}_2$  and diesel ICE.

## 5 Outlook and conclusion

In this study, a dual mode strategy was investigated to achieve high-power output while simultaneously limiting the  $\text{NO}_x$  emissions. The presented engine is a three-cylinder gasoline-based engine with Variable Turbine Geometry (VTG) and Variable Valve Timing (VVT). The engine operates in three distinct zones: part-load lean, high-load stoichiometric, and transient phases. In the part-load lean zone, a lean quality control strategy is implemented, while in the high-load stoichiometric zone, quantitative control is achieved through closed-loop lambda control.

The study highlights that:

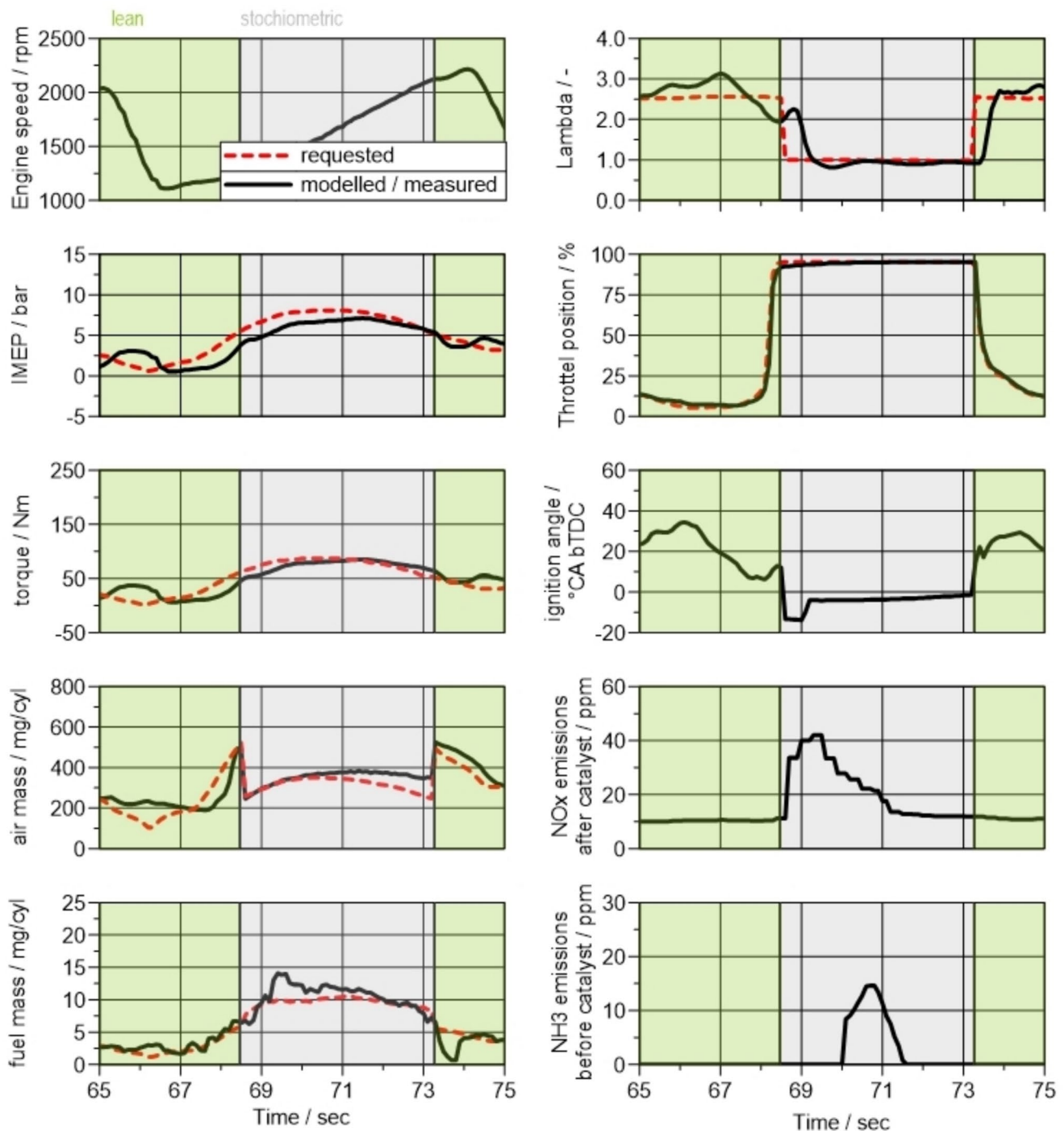


**Fig. 6** Load ramp with ignition angle retardation

- Nitrogen oxide emissions remain below  $c_{NO_x} = 100$  ppm in the lean operating range.
- During stoichiometric operation, a three-way catalytic converter effectively reduces emissions.
- Furthermore, software optimization has led to an impressive reduction of  $NO_x$  emissions by  $\Delta_{NO_x} = 84\%$ , achieving values as low as

$EF_{NO_x} = 102$  mg/km in the Worldwide Harmonized Light Vehicles Test Cycle (WLTC).

- The potential for further emission reductions through additional exhaust aftertreatment strategies is also discussed.

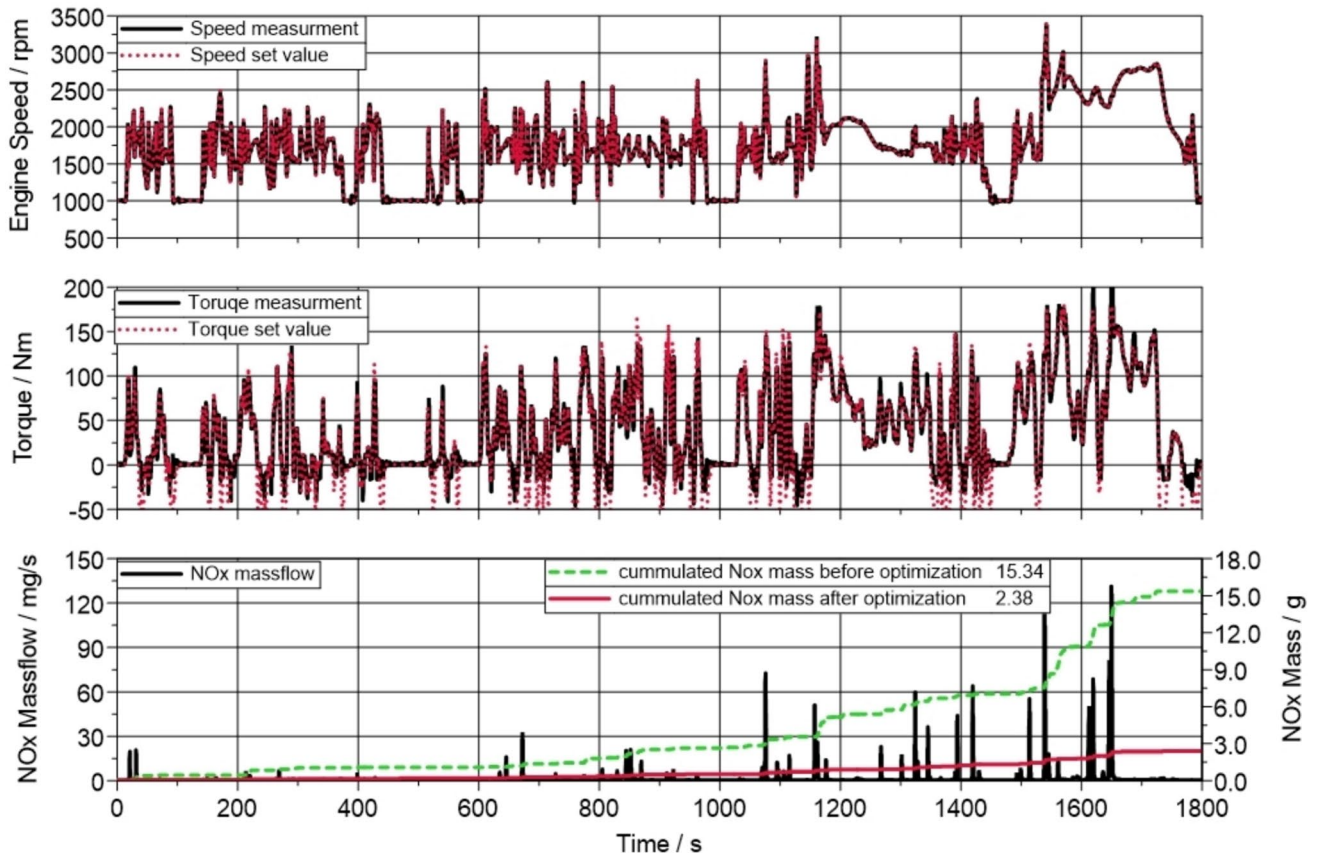


Fig. 7 WLTC with optimized strategy

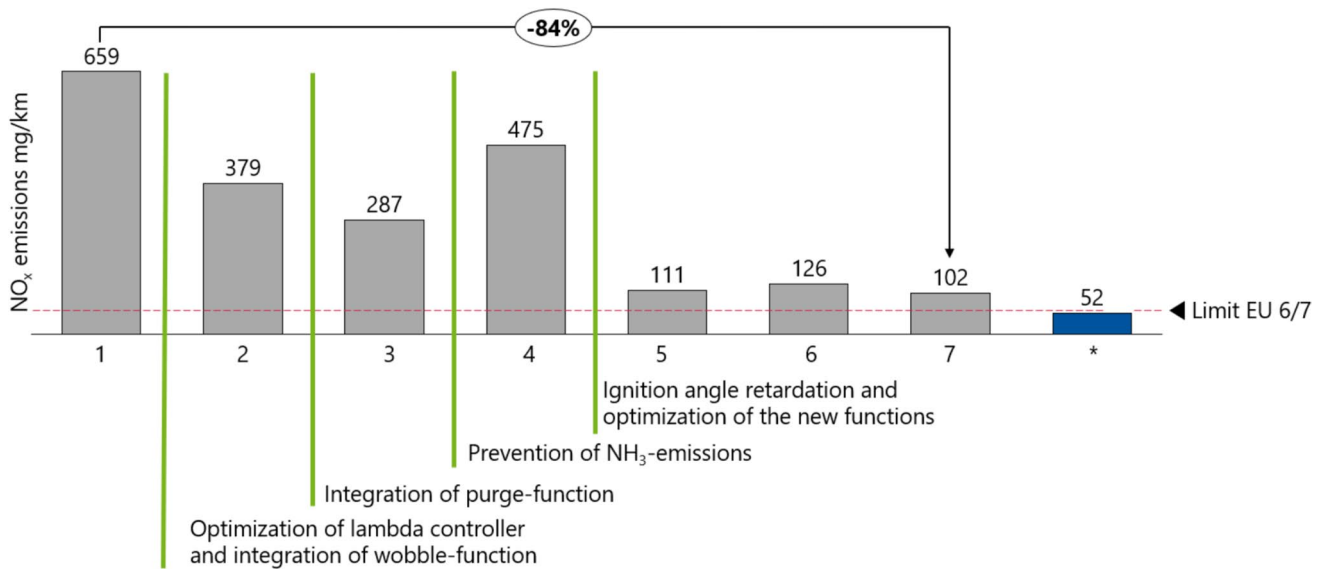
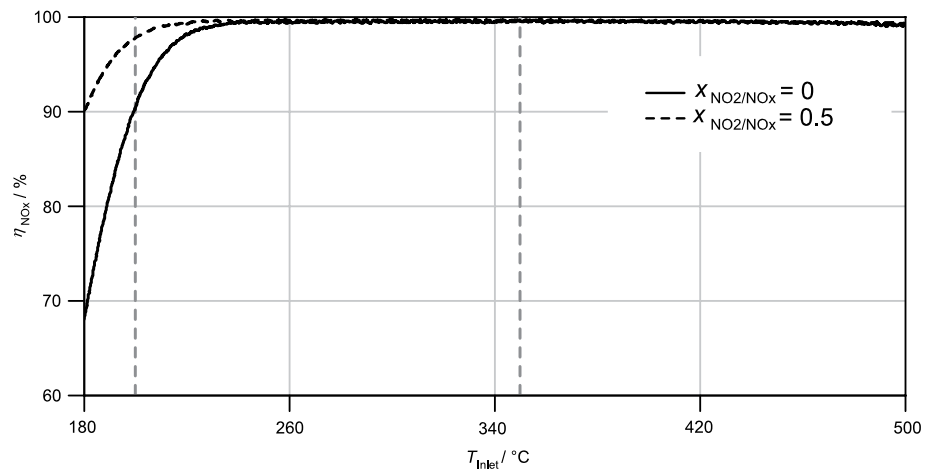


Fig. 8 NO<sub>x</sub> emission reduction potential due to the calibration of existing functions and implementing of new functions

These results demonstrate the effectiveness of the dual-mode strategy in reducing NO<sub>x</sub> emissions while maintaining high power output. Future work should focus on integrating additional optimizations and exhaust aftertreatment

technologies to further reduce emissions and improve the environmental performance of the powertrain. Therefore, the objective is to develop a highly innovative exhaust aftertreatment system and control concept that reduces

**Fig. 9** Comparison of the  $\text{NO}_x$  conversion efficiency  $\eta_{\text{NO}_x}$  of a Cu-SSZ-13 catalyst at different  $\text{NO}_2/\text{NO}_x$  ratios  $x_{\text{NO}_2}/\text{NO}_x$  during temperature programmed reaction (TPR). Exhaust gas specifications:  $\text{GHSV} = 50,000 \text{ h}^{-1}$ ,  $T_{\text{Inlet}} = 180\text{--}500 \text{ }^\circ\text{C}$ ,  $\psi_{\text{H}_2\text{O}} = 15\%$ ,  $\psi_{\text{NO}_x} = 500 \text{ ppm}$ ,  $x_{\text{NO}_2}/\text{NO}_x = 0$  and  $0.5$ ,  $\psi_{\text{NH}_3} = 750 \text{ ppm}$ ,  $\psi_{\text{O}_2} = 13\%$ , gases are balanced with  $\text{N}_2$



emissions of nitrogen oxides, ammonia, and nitrous oxide to levels classified as Zero-Impact Emissions. Special attention will be given to adapting supplier components such as turbochargers and catalyst to the specific characteristics of hydrogen as well as developing functions for the optimal operation of the catalyst, including heating strategies, and testing them on engine test benches.

**Supplementary Information** The online version contains supplementary material available at <https://doi.org/10.1007/s41104-025-00160-y>.

**Author contributions** Katrin Himmelseher: Writing—original draft preparation, Methodology, Investigation, Software. Alexander Lampkowski: Writing—original draft preparation, Investigation. Stefan Sterlepper: Writing—review & editing, Funding acquisition. Volker Müller: Writing—review & editing, Software, Methodology. Carole Querel: Software, Methodology. Joschka Schaub: Writing—review & editing. Dennis Lorei: Methodology, Investigation. Olaf Brüning: Methodology, Investigation. Claudia Conée: Methodology, Resources. Helmut Ruhland: Methodology, Resources. Marco Günther: Project administration, Funding acquisition. Stefan Pischinger: Supervision, Resources, Funding acquisition.

**Funding** Open Access funding enabled and organized by Projekt DEAL. This work was funded by the Federal Ministry of Research, Technology and Space (BMFTR) as part of the Hydrogen Clusters-4Future under the grant number 03ZU1115GA. The presented research work was carried out at the Center for Mobile Propulsion (CMP) of RWTH Aachen University with funding by the German Wissenschaftsrat (WR, Science Council) and the Deutsche Forschungsgemeinschaft (DFG, German Research Foundation) under the grant number INST 222/940-1 FUGB.

**Availability of data and materials** The data supporting the findings of this study are available within the paper and its Supplementary Information files. The dataset contains the test bench measurements of the shown experimental results.

## Declarations

**Competing interests** The authors declare no competing interests.

**Open Access** This article is licensed under a Creative Commons Attribution 4.0 International License, which permits use, sharing, adaptation, distribution and reproduction in any medium or format, as long as you give appropriate credit to the original author(s) and the source, provide a link to the Creative Commons licence, and indicate if changes were made. The images or other third party material in this article are included in the article's Creative Commons licence, unless indicated otherwise in a credit line to the material. If material is not included in the article's Creative Commons licence and your intended use is not permitted by statutory regulation or exceeds the permitted use, you will need to obtain permission directly from the copyright holder. To view a copy of this licence, visit <http://creativecommons.org/licenses/by/4.0/>.

## References

1. Akal, D., Öztuna, S., Büyükkakın, M.K.: A review of hydrogen usage in internal combustion engines (gasoline-Lpg-diesel) from combustion performance aspect. *Int. J. Hydrogen Energy* **45**(60), 35257–35268 (2020). <https://doi.org/10.1016/j.ijhydene.2020.02.001>
2. Aoyama, S., Sok, R., Kusaka, J.: Experimental and numerical analysis on the effect of adsorbed oxygen on the improvement of three-way catalysts purification performance by rich-lean lambda perturbation. *Fuel* **391**, 134816 (2025)
3. Beccari, S., Pipitone, E., Caltabellotta, S.: Analysis of the combustion process in a hydrogen-fueled CFR engine. *Energies* **16**(5), 2351 (2023). <https://doi.org/10.3390/en16052351>
4. Defoort, M., Olsen, D., Willson, B.: The effect of air-fuel ratio control strategies on nitrogen compound formation in three-way catalysts. *Int. J. Engine Res.* **5**(1), 115–122 (2004). <https://doi.org/10.1243/146808704772914291>
5. Eichlseder, H., Wallner, T., Freymann, R., et al.: The potential of hydrogen internal combustion engines in a future mobility scenario. In: Eichlseder, H., Wallner, T., Freymann, R., Ringler, J. (eds.) *JSAE Technical Paper Series*. Costa Mesa, California, United States: SAE International, PA, United States
6. Frasci, E., Sementa, P., Arsie, I., Jannelli, E., Vaglieco, B.M.: Experimental and numerical investigation of the impact of the pure hydrogen fueling on fuel consumption and  $\text{NO}_x$  emissions in a small DI SI engine. *Int. J. Engine Res.* **24**(8), 3574–3587 (2023). <https://doi.org/10.1177/14680874231162141>
7. Genovese, M., Fragiaco, P.: Hydrogen refueling station: overview of the technological status and research enhancement. *J.*

- Energy Storage **61**, 106758 (2023). <https://doi.org/10.1016/j.est.2023.106758>
8. Gong, C., Na, H., Kim, H., Yun, S., Cho, H., Won, W.: Energy-efficient and sustainable design of a hydrogen refueling station utilizing the cold energy of liquid hydrogen. *ACS Sustainable Chem. Eng.* **12**(37), 13763–13773 (2024). <https://doi.org/10.1021/acssuschemeng.4c01921>
  9. Goyal, H., Jones, P., Bajwa, A., Parsons, D., Akehurst, S., Davy, M.H., Leach, F.C.P., Esposito, S.: Design trends and challenges in hydrogen direct injection (H2DI) internal combustion engines—a review. *Int. J. Hydrogen Energy* **86**, 1179–1194 (2024). <https://doi.org/10.1016/j.ijhydene.2024.08.284>
  10. Greene, D.L., Ogden, J.M., Lin, Z.: Challenges in the designing, planning and deployment of hydrogen refueling infrastructure for fuel cell electric vehicles. *eTransportation* **6**, 100086 (2020). <https://doi.org/10.1016/j.etrans.2020.100086>
  11. Haas, M.: Just air? UniAir—the first fully-variable, electro-hydraulic valve control system. Schaeffler Symposium 2010. <http://www.bing.com/ck/a?!%26%26p=572f4a07d37715a2a10e75dad6287d711d7b3f53c8e1896f75dab4bd10c94f4JmltdHM9MTc1Mjc5NjgwMA%26ptn=3%26ver=2%26hsh=4%26clid=31b2b692-bb61-64eb-0167-a5d2ba3565af%26psq=schaeffler+symposium+uni+air%26u=a1aHR0cHM6Ly93d3cuc2NoYWVmZmxlcj5jb20vcvMvVtb3RlbWVkaWVuL2l1ZGhL19zaGFyZWZWRfbWVkaWEvMDhfbWVkaWFfbGlicmFyeS8wMV9wdWJsaWNhdGlvbnMvc2NoYWVmZmxlcj8yL3N5bXBvc2lhXzEvZGV93bmxvYWRzXzExL1NjaGFIZmZsZXJFS29sbG9xdWI1bV8yMDEwXzE4X2VuLnBkZg%26ntb=1>
  12. Himmelseher, K., Schaub, J., Müller, V.G., Geiger, S.M.: Optimization of emission behavior for a hydrogen combustion engine. *Hg. v. 33. Aachen Colloquium Sustainable Mobility*. 33. Aachen Colloquium Sustainable Mobility, Aachen (2024)
  13. Huang, M., Luo, Q., Sun, B., Zhang, S., Wang, K., Bao, L., Li, Q., Tang, X., Deng, W.: Experimental investigations of the hydrogen injectors on the combustion characteristics and performance of a hydrogen internal combustion engine. *Sustainability* **16**(5), 1940 (2024). <https://doi.org/10.3390/su16051940>
  14. Ihsan Shahid, M., Rao, A., Farhan, M., Liu, Y., Ahmad Salam, H., Chen, T., Ma, F.: Hydrogen production techniques and use of hydrogen in internal combustion engine: a comprehensive review. *Fuel* **378**, 132769 (2024). <https://doi.org/10.1016/j.fuel.2024.132769>
  15. Karim, G.: Hydrogen as a spark ignition engine fuel. *Int. J. Hydrogen Energy* **28**(5), 569–577 (2003). [https://doi.org/10.1016/S0360-3199\(02\)00150-7](https://doi.org/10.1016/S0360-3199(02)00150-7)
  16. Lai, F.-Y., Sun, B.-G., Zhang, Z.-F., Zhang, S.-W., Wang, K.-D., Ju, X.-M., Luo, Q.-H., Bao, L.-Z., Leach, F.: Experimental investigation of the matching boundary and optimization strategy of a variable geometry turbocharged direct-injected hydrogen engine. *Fuel* **373**, 132288 (2024). <https://doi.org/10.1016/j.fuel.2024.132288>
  17. Lee, S.W., Baek, H.-k., Lee, K.: Potential of hydrogen internal combustion engine for the decarbonised passenger vehicle. *Johnson Matthey Technol. Rev.* **68**(2), 293–303 (2024). <https://doi.org/10.1595/205651324X16965074891718>
  18. Luo, Q.-H., Sun, B.-G.: Inducing factors and frequency of combustion knock in hydrogen internal combustion engines. *Int. J. Hydrogen Energy* **41**(36), 16296–16305 (2016). <https://doi.org/10.1016/j.ijhydene.2016.05.257>
  19. Medda, M., Calia, V., Di Sacco, M., Gullino, F., Rossi, V., Silvestri, N., Tonelli, R., Zaffino, F.: Challenges and opportunities in developing a H<sub>2</sub> high specific power turbo-charged engine. In: 32nd Aachen Colloquium Sustainable Mobility 2023. Aachen, Paper No. 066 (2023)
  20. Misul, D.A., Scopelliti, A., Baratta, M.: High-performance hydrogen-fueled internal combustion engines: feasibility study and optimization via 1D-CFD modeling. *Energies* **17**(7), 1593 (2024). <https://doi.org/10.3390/en17071593>
  21. Müller, V., Gottorf, S., Schaub, J., Virnich, L.: Modulare H<sub>2</sub>-Motorsteuerung. *MTZ Motortechnische Z.* **83**(9), 16–25 (2022). <https://doi.org/10.1007/s35146-022-0846-2>
  22. Nguyen, D., Kar, T., Turner, J.W.G.: Performance, emissions, and combustion characteristics of a hydrogen-fueled spark-ignited engine at different compression ratios: experimental and numerical investigation. *Energies* **16**(15), 5730 (2023). <https://doi.org/10.3390/en16155730>
  23. Özyalcin, C., Mauermann, P., Dirkes, S., Thiele, P., Sterlepper, S., Pischinger, S.: Investigation of filtration phenomena of air pollutants on cathode air filters for PEM fuel cells. *Catalysts* **11**(11), 1339 (2021). <https://doi.org/10.3390/catal11111339>
  24. Özyalcin, C., Sterlepper, S., Roiser, S., Eichlseder, H., Pischinger, S.: Exhaust gas aftertreatment to minimize NO<sub>x</sub> emissions from. *Appl. Energy* **353**(Part A), 122045 (2024). <https://doi.org/10.1016/j.apenergy.2023.122045>
  25. Peters, N., Bunce, M.: Lambda determination challenges for ultra-lean hydrogen-fueled engines and the impact on engine calibration. In: Bunce, M., Peters, N. (eds.) SAE Technical Paper Series. WCX SAE World Congress Experience. SAE International 400 Commonwealth Drive, Warrendale, PA, united states (SAE technical paper series), Detroit, MI (2023)
  26. Ricci, F., Zemi, J., Avana, M., Grimaldi, C.N., Battistoni, M., Papi, S.: Analysis of hydrogen combustion in a spark ignition research engine with a barrier discharge igniter. *Energies* **17**(7), 1739 (2024). <https://doi.org/10.3390/en17071739>
  27. Rottengruber, H., Berckmüller, M., Elsässer, G., Brehm, N., Schwarz, C.: Direct-injection hydrogen si-engine—operation strategy and power density potentials. *SAE Trans.* **113**, 1749–1761 (2004)
  28. Seba, B., Weiss, U.: The development of a 6-cylinder hydrogen engine for the off-highway market. In: Heintzel, A. (ed.) *Heavy-Duty-, On- und Off-Highway-Motoren 2022. Stand der Energiewende im Heavy-Duty-Bereich*, pp. 13–23. Springer, Wiesbaden (2023)
  29. Sementa, P., de Vargas Antolini, J.B., Tornatore, C., Catapano, F., Vaglieco, B.M., López Sánchez, J.J.: Exploring the potentials of lean-burn hydrogen SI engine compared to methane operation. *Int. J. Hydrogen Energy* **47**(59), 25044–25056 (2022). <https://doi.org/10.1016/j.ijhydene.2022.05.250>
  30. Sterlepper, S., Lampkowski, A., Himmelseher, K., Özyalcin, C., Claßen, J., Pischinger, S.: The role of hydrogen in exhaust gas aftertreatment systems of hydrogen combustion engines. In: Sterlepper, S., Lampkowski, A., Himmelseher, K., Özyalcin, C., Claßen, J., Pischinger, S. (eds.) SAE Technical Paper Series. WCX SAE World Congress Experience. SAE International 400 Commonwealth Drive, Warrendale, PA, USA (SAE technical paper series), Detroit, MI (2025)
  31. Terhorst-Kluge, K.A., Himmelseher, K., Müller, V., Querel, C., Heimowski, P., Günther, M., Basler, M., Pischinger, S., Abel, D., Vallery, H.: Optimal control of an over-actuated spark-ignited hydrogen engine. *Int. J. Hydrogen Energy* **145**, 267–279 (2025). <https://doi.org/10.1016/j.ijhydene.2025.05.171>
  32. Turner, J.W.G.: Future technological directions for hydrogen internal combustion engines in transport applications. *Appl. Energy Combust. Sci.* **21**, 100302 (2025). <https://doi.org/10.1016/j.jaecs.2024.100302>
  33. Uchida, N., Onorati, A., Novella, R., Agarwal, A.K., Abdul-Manan, A.F.N., Kulzer, A.C., Di Iorio, S., Gordillo, V., Günther, M., Jena, A., Lucchini, T., Payri, R., Pesyridis, A., Vaglieco, B.M., Valera, H.: E-fuels in IC engines: a key solution for a future decarbonized transport. *Int. J. Engine Res.* **26**(11), 1675–1702 (2025). <https://doi.org/10.1177/14680874251325296>

34. Verhelst, S., Wallner, T.: Hydrogen-fueled internal combustion engines. *Prog. Energy Combust. Sci.* **35**(6), 490–527 (2009). <https://doi.org/10.1016/j.pecs.2009.08.001>
35. Wallner, T., Lohsebusch, H., Gurski, S., Duoba, M., Thiel, W., Martin, D., Korn, T.: Fuel economy and emissions evaluation of BMW Hydrogen 7 mono-fuel demonstration vehicles. *Int. J. Hydrogen Energy* **33**(24), 7607–7618 (2008). <https://doi.org/10.1016/j.ijhydene.2008.08.067>
36. Webster, L.J., Ballard, R., Beamish, T., Burnhope, T., Humbert, J., Lewis, A.C., Piaszyk, J., Moller, S.J.: Evaluating low NO<sub>x</sub> hydrogen engines designed for off-road and construction applications. *Environ Sci Process Impacts* **27**(2), 486–497 (2025). <https://doi.org/10.1039/d4em00448e>
37. Wei, H., Hu, Z., Ma, J., Ma, W., Yuan, S., Hu, Y., Hu, K., Zhou, L., Wei, H.: Experimental study of thermal efficiency and NO<sub>x</sub> emission of turbocharged direct injection hydrogen engine based on a high injection pressure. *Int. J. Hydrogen Energy* **48**(34), 12905–12916 (2023). <https://doi.org/10.1016/j.ijhydene.2022.12.031>
38. Wolkenar, B., Schönebaum, S., Mauermann, P., Dittmann, P., Pischinger, S., Simon, U.: Storage and oxidation of oxygen-free and oxygenated hydrocarbons on a Pt–Pd series production oxidation catalyst. *Top. Catal.* **62**(1–4), 376–385 (2019). <https://doi.org/10.1007/s11244-018-1109-9>
39. Yavuz, M., Brinklow, G., Cova Bonillo, A., Herreros, J.M., Wu, D., Doustdar, O., Zeraati-Rezaei, S., Tsolakis, A., Millington, P., Alcove Clave, S.: The suitability of the three-way catalyst for hydrogen fuelled engines. *Johnson Matthey Technol. Rev.* **68**(3), 412–426 (2024). <https://doi.org/10.1595/205651324X17054113843942>
40. Yip, H.L., Srna, A., Zhai, G., Wehrfritz, A., Kook, S., Hawkes, E.R., Chan, Q.N.: Laser-induced plasma-ignited hydrogen jet combustion in engine-relevant conditions. *Int. J. Hydrog. Energy* **48**(4), 1568–1581 (2023). <https://doi.org/10.1016/j.ijhydene.2022.09.296>
41. Zhao, N., Liu, Z., Wang, L., Pan, J., Huang, Z.: Experimental study on performance and emission of an electric turbocharged hydrogen direct injection engine. *ACS Omega* **9**(25), 27407–27414 (2024). <https://doi.org/10.1021/acsomega.4c02222>

**Publisher's Note** Springer Nature remains neutral with regard to jurisdictional claims in published maps and institutional affiliations.